Schizophrenia Research 208 (2019) 242–249

Contents lists available at ScienceDirect

Schizophrenia Research

journal homepage: www.elsevier.com/locate/schres

Positive and general psychopathology associated with specific gray matter reductions in inferior temporal regions in patients with schizophrenia

Eva Mennigen [a,1], Wenhao Jiang [b,*,1], Vince D. Calhoun [c], Theo G.M. van Erp [d], Ingrid Agartz [e], Judith M. Ford [f,g], Bryon A. Mueller [h], Jingyu Liu [c], Jessica A. Turner [b]

[a] Department of Psychiatry and Biobehavioral Sciences, University of California, Los Angeles, Los Angeles, CA, USA
[b] Department of Psychology, Georgia State University, Atlanta, GA, USA
[c] The Mind Research Network, Albuquerque, NM, USA
[d] Clinical Translational Neuroscience Laboratory, Department of Psychiatry and Human Behavior, University of California, Irvine, CA, USA
[e] NORMENT, KG Jebsen Centre for Psychosis Research, Division of Mental Health and Addiction, University of Oslo, Oslo, Norway
[f] San Francisco Veterans Administration Medical Center, San Francisco, CA, USA
[g] Department of Psychiatry, University of California, San Francisco, San Francisco, CA, USA
[h] Department of Psychiatry and Behavioral Sciences, University of Minnesota, Minneapolis, MN, USA

ARTICLE INFO

Article history:
Received 16 November 2018
Received in revised form 8 February 2019
Accepted 18 February 2019
Available online 26 February 2019

Keywords:
Parallel independent component analysis
Gray matter alterations
Schizophrenia
Positive and negative syndrome scale
Inferior temporal gyrus

ABSTRACT

Schizophrenia is a complex disorder that affects perception, cognition, and emotion causing symptoms such as delusions, hallucinations, and suspiciousness. Schizophrenia is also associated with structural cortical abnormalities including lower gray matter (GM) concentration, GM volume, and cortical thickness relative to healthy control individuals. However, the association between GM measures and symptom dimensions in schizophrenia is still not well understood.

Here, we applied parallel independent component analysis (pICA), a higher-order statistical approach that identifies covarying patterns within two (or more) data modalities simultaneously, to link covarying brain networks of GM concentration with covarying linear combinations of the positive and negative syndrome scale (PANSS). In a large sample of patients with schizophrenia (n = 337) the association between these two data modalities was investigated.

The pICA revealed a distinct PANSS profile characterized by increased delusional symptoms, suspiciousness, hallucinations, and anxiety, that was associated with a pattern of lower GM concentration in inferior temporal gyri and fusiform gyri and higher GM concentration in the sensorimotor cortex. GM alterations replicate previous findings; additionally, applying a multivariate technique, we were able to map a very specific symptom profile onto these GM alterations extending our understanding of cortical abnormalities associated with schizophrenia. Techniques like parallel ICA can reveal linked patterns of alterations across different data modalities that can help to identify biologically-informed phenotypes which might help to improve future treatment targets.

1. Introduction

Schizophrenia can be conceptualized as a neurodevelopmental disorder encompassing altered maturation of brain structure and function that can be captured in vivo by magnetic resonance imaging (MRI) (Birnbaum and Weinberger, 2017; Bora, 2015; Gur et al., 2014; Murray et al., 2017; Satterthwaite et al., 2015). With regard to brain structure, previous studies in patients with schizophrenia have not only found widespread disruptions of white matter microstructure and fiber tracts, but they also found that gray matter (GM) properties such as GM volume, GM concentration, cortical thickness, and cortical surface area are affected in individuals with schizophrenia (Samartzis et al., 2014; Sun et al., 2015; Zhang et al., 2016).

Lower GM concentration, as measured with voxel-based morphometry (VBM) (Ashburner and Friston, 2000) or source-based morphometry (SBM), its multivariate extension (Xu et al., 2009), in patients with schizophrenia relative to healthy control individuals have been identified in brain regions associated with the salience network, such as the insular cortex and the dorsal anterior cingulate cortex (ACC), in the left parahippocampal gyrus and inferior frontal gyrus, as well as in the basal ganglia (Fornito et al., 2009; Glahn et al., 2008; Gupta et al.,

* Corresponding author at: Imaging Genetics and Informatics Laboratory, Department of Psychology, Georgia State University, Atlanta, GA, USA.
E-mail address: wjiang5@student.gsu.edu (W. Jiang).
[1] These authors contributed equally.

https://doi.org/10.1016/j.schres.2019.02.010
0920-9964/

2015). Underlining neurodevelopmental aspects of schizophrenia, and more generally of the psychosis spectrum, Satterthwaite and colleagues recently demonstrated that structural abnormalities like lower GM volume are already present in youth experiencing subclinical levels of psychotic symptoms (Satterthwaite et al., 2016).

However, schizophrenia presents clinically with a heterogeneous range of symptoms including abnormalities of perception, cognition, and emotion (American Psychiatric Association and others, 2003). Therefore, it seems important to investigate the association between symptom dimensions and structural changes in order to gain a precise understanding of the pathophysiology underlying schizophrenia. Accordingly, many studies have investigated whether one of the most prevalent symptoms in schizophrenia, i.e., auditory hallucinations (Andreasen and Flaum, 1991), corresponds to structural changes. In region of interest and whole brain analyses of structural MRI data, it has been demonstrated that auditory hallucinations are associated with cortical thinning in auditory cortices (superior and middle temporal gyri, Heschl's gyri) (Cui et al., 2018; Modinos et al., 2013; Mørch-Johnsen et al., 2017). Even though auditory hallucinations are indeed a very common symptom in schizophrenia with a prevalence of >70% (Shinn et al., 2012), it does not fully reflect the complexity of symptoms characterizing schizophrenia.

The positive and negative syndrome scale (PANSS) (Kay et al., 1987) is one of the most commonly used questionnaires to assess symptomatology in patients with schizophrenia and it allows for the investigation of dimension-specific abnormalities. Koutsouleris et al. (2009) investigated the associations between VBM-derived GM concentration measures and the three PANSS dimensions summarizing positive, negative, and general symptoms. GM concentration showed a negative association with all three PANSS dimensions though the negative domain showed the most widespread effects. They found that GM concentration in the temporal cortex, the thalamus, insula, inferior frontal gyri, medial and lateral prefrontal cortices, and the ACC was associated with all three dimensions. A recent mega-analysis of GM concentration in patients with schizophrenia (n = 784), compared VBM vs. SBM analyses and associations between GM concentration and PANSS positive and negative scores were investigated post hoc (Gupta et al., 2015). Generally, previously described brain areas of lower GM concentration in schizophrenia were confirmed (temporal lobe, insula, medial frontal lobe) with high overlap between VBM and SBM analyses. However, reduced GM concentration was not significantly associated with either positive or negative PANSS dimension scores.

In summary, even though there seems to be a consensus on the *general* regions of lower GM concentration associated with schizophrenia, the mapping of schizophrenia symptomatology onto specific brain alterations has yielded inconsistent findings. Most previous studies have calculated associations between symptoms and GM measures using predefined brain regions, on the one hand, and PANSS total or factor scores, on the other hand. Even though these approaches are informative, they might lack sensitivity to detect alterations associated with specific symptoms or clusters of symptoms.

One approach to overcome these shortcomings is to apply higher-order statistical techniques like parallel independent component analysis (pICA) which identifies patterns of alterations within two or more modalities (Calhoun and Sui, 2016; Liu et al., 2009; Liu and Calhoun, 2007; Pearlson et al., 2015; Vergara et al., 2014). ICA, as a special case of blind source separation, identifies maximally independent components within one data modality. The extension to this algorithm, pICA, performs individual ICA on multiple data modalities, 'in parallel', maximizing independence within each modality, while additionally optimizing for correlation of independent components between the data modalities. As a result of this type of analysis, correlation coefficients between independent components of the two modalities are estimated and individuals' loading coefficients for each independent component can then be used to further interrogate group differences. A recent study employing pICA on functional connectivity measures of the default mode network (DMN) and genetic data found that genes regulating neurodevelopmental processes are associated with functional hypoconnectivity of the DMN in patients with schizophrenia (Meda et al., 2014). By applying pICA, this study provided meaningful insights into the etiology of schizophrenia encouraging further multimodal investigations.

Here, we performed pICA on GM concentration images and PANSS items in an aggregated sample of patients with schizophrenia (n = 342). Since associations between GM measures and symptom scores tend to be weak, large samples or the combination of data from multiple samples are needed to provide sufficient power in order to identify such relationships. We hypothesized that (i) pICA would roughly identify established symptom dimensions of PANSS scores, i.e., positive, negative, and general, and (ii) that temporal and prefrontal brain areas would show associations with distinct PANSS components reflecting recent findings of GM volume and cortical thickness (Padmanabhan et al., 2015).

2. Material and methods

2.1. Participants

Data were pooled from three major studies: TOP (Thematic Organized Psychosis research; Oslo, Norway) (Athanasiu et al., 2010), FBIRN 3 (Functional imaging Biomedical Information Research Network, multiple sites in the USA) (Potkin et al., 2009; Wible et al., 2009), and COBRE (Center of Biomedical Research Excellence, Albuquerque, NM, USA) (Aine et al., 2017; Turner et al., 2012). Data were collected under approval of local institutional review boards and all participants provided informed consent.

All studies provided structural MRI data as well as PANSS item scores. In total, data were obtained from 342 patients with a diagnosis of schizophrenia or schizoaffective disorder as confirmed by the Structured Clinical Interview for Diagnosis (SCID) for DSM-IV or DSM-IV-TR conducted at each study site (First and Gibbon, 2004). All studies provided information on age at time of scan, sex, duration of illness, and medication status (in varying detail) for each participant.

Demographic and scanning information are presented in Table 1.

2.2. Positive and negative symptom scores (PANSS)

Since data were drawn from independent (multi-center) studies and because sample mean age and illness duration differed significantly between studies, potential confounding effects of study site and illness duration on PANSS scores were explored in a multivariate analysis of covariance (MANCOVA) framework: the 30 PANSS items (multivariate dependent variable) were tested for associations with study site (independent variable) while controlling for illness duration. In addition, the PANSS total score was tested for an association with study site controlling for illness duration employing analysis of co-variance (ANCOVA).

2.3. Preprocessing

T1-weighted structural MRI data were normalized to the standard Montreal Neurological Institute (MNI) template using a 12-parameter affine model, resliced to a voxel size of $2 \times 2 \times 2$ mm and segmented into GM, white matter, and cerebro-spinal fluid using Statistical Parametric Mapping 12 (SPM12, http://www.fil.ion.ucl.ac.uk/spm/software/spm12/), ending with normalized segmented images, prior to smoothing. To identify possible outliers, individual scans were correlated with the group-generated GM template and outliers were visually checked. Scans from 5 individuals showed low correlations with the group-generated GM template ($\rho < 0.98$) and were discarded; 337 participants were included in the subsequent analyses.

In order to account for possible effects of age, sex, and study site on structural MRI data, voxel-wise regression was applied to remove

Table 1
Demographic and scanning information.

	FBIRN 3 N = 156	TOP N = 110	COBRE N = 71	p-Value < 0.05
Age (in years)	39.4 ± 11.7[a]	30.9 ± 8.2[b]	36.7 ± 12.3[a]	TOP < FBIRN 3 and COBRE
Duration of illness (in years)	17.99 ± 11.8[a]	7.07 ± 6.3[b]	16.04 ± 12.0[a]	TOP < FBIRN 3 and COBRE
AP medication (in %)	95.6	88.2	91.5	n.s.
CPZ equivalent (in mg/d)	542.35 ± 1271.4	n/a	516.32 ± 1095.4	n.s.
PANSS total score	59.2 ± 14.6	61.8 ± 17	59.9 ± 14.3	n.s.
Field strength (in T)	3	1.5	3	
Sequence	MPRAGE	MPRAGE	MPRAGE	
Voxel size (mm)	1.1 × 0.9 × 1.2	1.33 × 0.94 × 1	1 × 1 × 1	
Scanning orientation	Sagittal	Sagittal	Sagittal	

AP – antipsychotic medication, CPZ – chlorpromazine equivalent: information was available for n = 129 FBIRN participants and for n = 70 COBRE participants. The superscript a and b indicated the result of ANOVA with post-hoc pairwise comparisons (with Bonferroni correction), TOP participants were significantly younger and showed shorter duration of illness than FBIRN3 and COBRE.
No significant group differences in AP medication, CPZ equivalent, and PANSS total score.

effects of these three variables. Finally, structural MRI data were smoothed with a 10 mm Gaussian kernel.

2.4. Parallel independent component analysis (pICA)

We used the fusion ICA Toolbox (FIT, http://mialab.mrn.org/software/fit/) to perform pICA on the smoothed, normalized structural MRI data and raw PANSS scores (30 items per participant). The minimum description length (MDL) algorithm estimated the optimal number of components to be 25 for the structural MRI data. Each PANSS item was designed to represent distinct psychopathological symptoms. However, to apply a high model order to PANSS scores would have resulted in difficulties in convergence between the two modalities. Considering the inner structure of the PANSS (positive, negative and general dimensions), the model order was set to three independent components. Importantly, a PANSS component derived from the ICA can reflect any combination of PANSS items based on the data itself and the three PANSS components do not necessarily reflect the preset inner structure.

Within the pICA framework, a GM mask to exclude the cerebellum (due to its low reliability across studies) was applied on structural MRI data before ICA was performed. To ensure stability of component estimation, infomax ICA was run 20 times, and the central point of 20 runs was selected as the final component using ICASSO (Bell and Sejnowski, 1995; Himberg and Hyvärinen, 2003).

Only the pair of GM component and PANSS component that showed the highest correlation was constrained in the analysis in order to yield more stable results. More specifically, the correlation between loading coefficients of this structural MRI – PANSS pair was enhanced through pICA while independence within each modality was further maximized.

All subsequent analyses were performed on the loading coefficients from this first component pair.

2.5. Validation tests

To further test stability of pICA estimation, we performed 10-fold validation to ensure that the pICA estimation was not driven by outliers. Each validation included 90% of the individuals of the sample and was balanced across different study sites. Parameter settings were the same as in the original analysis. The results from each iteration were examined for overlap, i.e., correlation, with the original pICA.

2.6. Post hoc analyses

Illness duration and medication status are typical confounders in studies involving patients with schizophrenia.

In a regression framework, possible effects of illness duration (predictor) on the loading coefficients of the structural MRI component and the PANSS component (dependent variable) were tested.

We tested for an effect of medication on both modalities' loading coefficients in the subsample of 199 participants for whom chlorpromazine (CPZ) equivalents were available; we applied Spearman's rho test because of a skewed distribution.

To further explore the relationship between the traditional PANSS dimension scores and the data-driven dimensions of the PANSS and structural MRI components derived from the pICA, correlation analyses were performed on PANSS positive, negative, and general scores and the loading coefficients of the components.

3. Results

3.1. Positive and negative syndrome scale (PANSS)

The PANSS total score did not differ significantly between sites of the three different studies after controlling for illness duration ($F = 1.57$, $df = 7$, $p = 0.14$). However, the MANCOVA revealed significant differences in several PANSS items (see Supplementary material). Importantly, items that contributed most to the PANSS component, including delusional symptoms (P1), suspiciousness/persecution (P6), and anxiety (G2), were not significantly associated with study site (see below and Supplementary material).

3.2. Parallel independent component analysis

The correlation between the structural MRI and PANSS components was Pearson's $r = 0.25$ ($p = 2.62 \times 10^{-06}$, Bonferroni-corrected

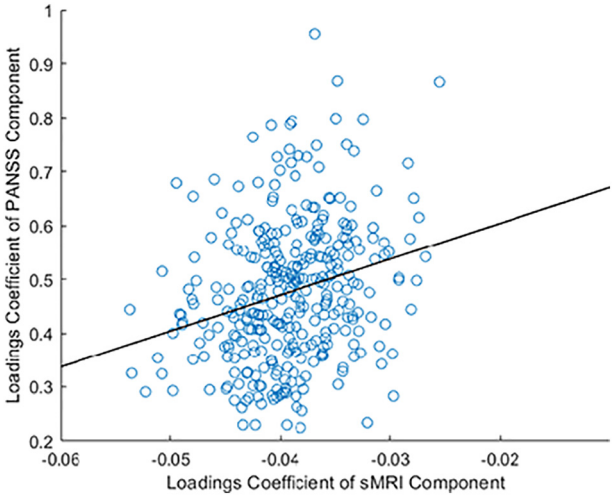

Fig. 1. Correlation between loading coefficients of the top PANSS component and the top structural MRI component. Pearson's $r = 0.25$, $p = 2.62 \times 10^{-06}$ (Bonferroni-corrected threshold $= 6.67 \times 10^{-04}$).

threshold = 6.67×10^{-04}) shown in Fig. 1. The 10-fold validation showed that results in 8 out of the 10 validation runs were consistent with findings of the original analysis. Given that the correlation was positive, individuals with greater structural loading coefficients for this component also showed greater symptom profile loadings.

The structural MRI component consisted of lower GM concentration in bilateral inferior temporal gyri merging with fusiform gyri and the gyrus rectus, and higher GM concentration in bilateral pre- and postcentral gyri (see Fig. 2a and Table 2).

The PANSS component was most strongly positively weighted on delusional symptoms (P1), hallucinatory behavior (P3), suspiciousness/persecution (P6), and anxiety (G2). Poor rapport (N3), mannerism and posturing (G5), uncooperativeness (G8), disorientation (G10), and disturbance of volition (13) were negatively associated with this component (Fig. 2b).

In summary, patients with higher reductions in inferior temporal gyri and fusiform gyri and increased GM concentration in pre- and postcentral gyri, also exhibit a more severe symptom profile consisting of higher delusional symptoms, suspiciousness, and anxiety and lower symptoms of mannerism, disorientation, and uncooperativeness.

The 10-fold validation showed high correlation with the original pICA run with a mean correlation of Pearson's r = 0.81; in 2 out of 10 validation runs the directionality of the structural MRI component and therefore its association with the PANSS component was inverted.

3.3. Post hoc analyses

The regression models including loading coefficients of the structural MRI component or PANSS component (dependent variable) and illness duration (predictor) showed no significant association (β_{sMRI}

a) Structural MRI component

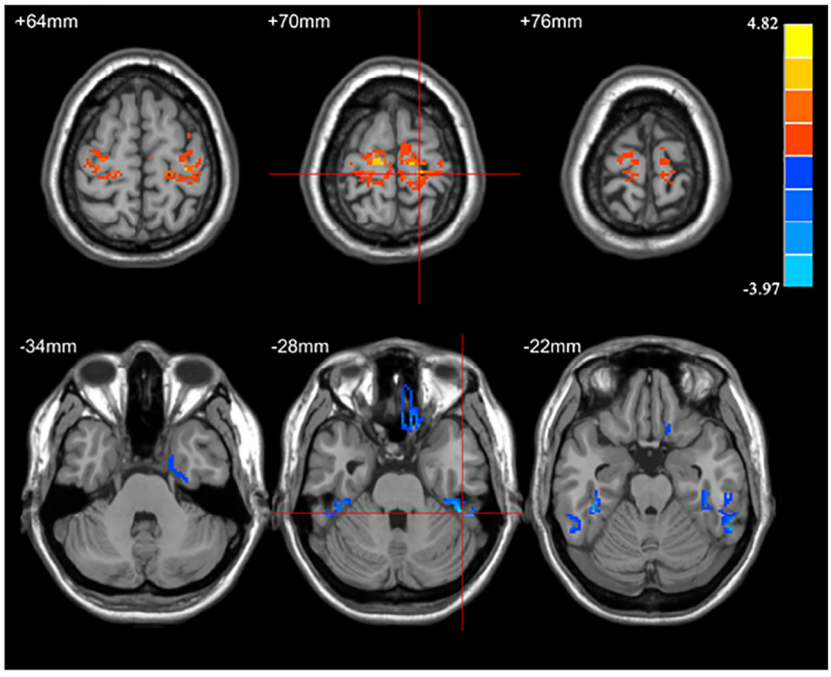

b) PANSS component

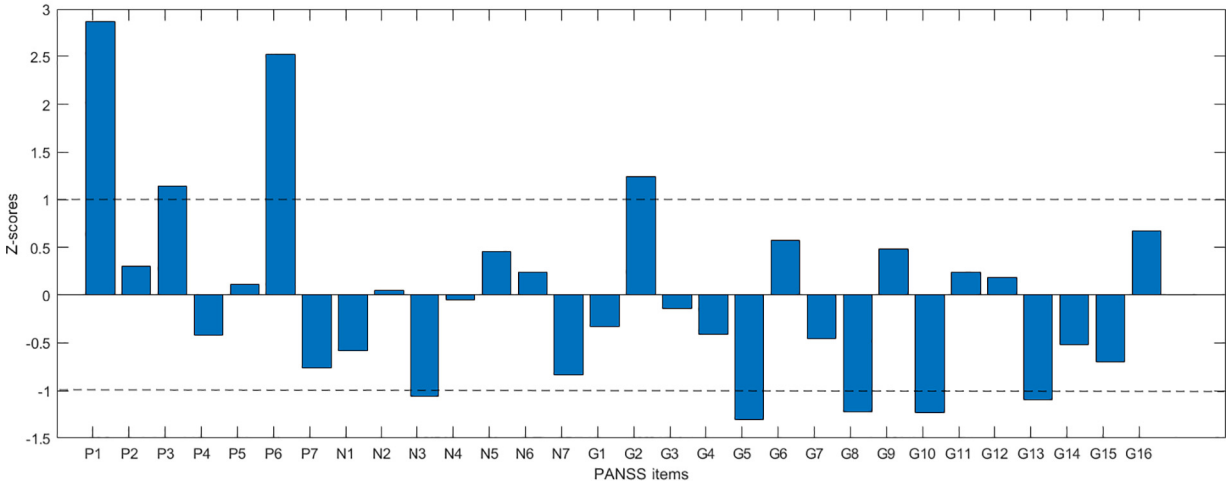

Fig. 2. Parallel ICA results - the top a) structural MRI and b) PANSS components. PANSS items with |Z| >1: P1 – delusion symptoms; P3 – hallucinatory behavior; P6 – suspiciousness/persecution; N3 – poor rapport; G2 – anxiety; G5 – mannerisms and posturing; G8 – uncooperativeness; G10 – disorientation; G13 – disturbance of volition.

Table 2
Brain regions, volumes and peak coordinates.

Structural MRI component	Brain regions	Volume (cc^3)	Brodmann area	Z-score and peak coordinates
Cluster 1	R fusiform gyrus	0.59	20, 36	−2.8 (22, 2, −40)
	R inferior temporal gyrus	0.44		
Cluster 2	R fusiform gyrus	0.83	20, 36, 37	−3.6 (46, −38, −28)
	R inferior temporal gyrus	1.6		
Cluster 3	L fusiform gyrus	0.85	20, 36, 37	−3.3 (−42, −34, −22)
	L inferior temporal gyrus	0.84		
Cluster 4	Rectal gyrus	0.78	11, 47	−3.0 (10, 26, −26)
Cluster 5	R precentral gyrus	3.2	3, 4, 6	3.8 (18, −28, 70)
	R postcentral gyrus	2.0		
Cluster 6	L precentral gyrus	2.5	3, 4, 6	4.0 (−12, −22, −72)
	L postcentral gyrus	0.5		

Z-threshold > 2, and clusters size > 150 voxel. L - left, R - right.

$= 0.25$, $t_{sMRI} = 0.45$, $p_{sMRI} = 0.65$; $\beta_{PANSS} = 0.03$, $t_{PANSS} = 0.62$, $p_{PANSS} = 0.54$).

Within the subsample with available CPZ equivalents there were no significant correlations between CPZ equivalents and the structural MRI loading coefficients (Spearman's $\rho = 0.08$, $p = 0.25$) or loading coefficients for the PANSS component (Spearman's $\rho = 0.12$, $p = 0.1$). CPZ equivalents did not differ significantly between the two studies providing these data ($t = -0.15$, $df = 197$, $p = 0.89$).

The correlation between the traditional PANSS dimension scores and the experimentally derived PANSS loading coefficients revealed high correlations with PANSS positive (Pearson's $r = 0.83$, $p < 0.001$), negative (Pearson's $r = 0.51$, $p < 0.001$), and general (Pearson's $r = 0.85$, $p < 0.001$) scores.

Likewise, loading coefficients of the structural MRI component were significantly correlated with PANSS positive (Pearson's $r = 0.23$, $p < 0.001$), negative (Pearson's $r = 0.14$, $p = 0.008$), and general (Pearson's $r = 0.22$, $p < 0.001$) scores.

4. Discussion

The brain structure underlying symptom presentation in schizophrenia is likely not a single region affecting a single symptom. Networks of regions are functionally related to single symptoms, and to groups of symptoms (Hare et al., 2017; Hare et al., 2018; Modinos et al., 2013; Shinn et al., 2012; Walton et al., 2017; Walton et al., 2018); we examined whether patterns of GM covariation (GM networks) related to patterns of symptoms (data-driven symptom dimensions) using the pICA approach (Liu and Calhoun, 2007). We identified a combination of positive and general symptoms correlated with GM measures in a network of inferior temporal and pre- and postcentral regions.

The PANSS component that correlated with the structural component differed from the traditional dimensions of the PANSS, i.e., positive, negative, and general; instead, delusional symptoms, hallucinations, suspiciousness, and anxiety contributed positively to the component, whereas mannerism, disorientation, and uncooperativeness contributed negatively. This pattern could be broadly described as symptomatology characteristic of a chronic form of the now obsolete schizophrenia subtype of paranoid schizophrenia: whereas positive symptoms such as delusions exist, they are not accompanied by symptoms that typically occur during the acute phase of schizophrenia (disorientation, uncooperativeness) (Tandon et al., 2013). Loading coefficients of this PANSS component correlated strongly with the PANSS general and positive scores, indicating that individuals with more severe overall symptoms also showed higher loading coefficients for this component.

As for the structural MRI data, the component included GM concentrations of temporal (inferior and posterior medial), frontal (precentral gyri and gyrus rectus), and parietal brain areas (postcentral gyri). Specifically, this component was associated with lower GM concentration in inferior temporal regions and higher GM concentration in sensorimotor areas.

In general, lower GM concentration as often observed in patients with schizophrenia can presumably not only derive from reductions in neuron density (Harrison, 1999; Todtenkopf et al., 2005) but can also be due to changes in the glia compartment (Fornito et al., 2009). Even though lower GM concentration and cortical thickness often parallel each other (Narr et al., 2005), it may be that they reflect different pathophysiological processes (Fornito et al., 2009). Further, these reductions might be, at least partially, caused by treatment with antipsychotic medication (Huhtaniska et al., 2017; Vita et al., 2015). However, post-hoc analyses did not reveal a significant association between loading coefficients of the structural component and CPZ equivalents.

Interestingly, anatomical regions identified here parallel previous multivariate findings of lower cortical thickness and GM volume in an independent sample of patients with schizophrenia; Padmanabhan et al. (2015) applied exploratory factor analyses to structural measures (GM volume, cortical thickness and surface area) of regions that showed a general association with the PANSS positive scale. They identified, amongst others, a temporal factor that included the cortical thickness of bilateral inferior temporal gyri as well as bilateral fusiform gyri; this factor was a significant predictor of PANSS positive scores (Padmanabhan et al., 2015). In the current study we show similar alterations in GM concentration in inferior temporal gyri and fusiform gyri with a different multivariate approach. We also expand on the distinct symptom profile consisting of specific positive, negative, and general symptoms associated with these structural alterations. Generally, the inferior temporal gyri and fusiform gyri have long been associated with object and face/body recognition (Gerlach et al., 2002; Kim et al., 2014). In individuals with schizophrenia, alterations in morphology of inferior temporal and fusiform gyri have been more specifically associated with impairments in spatial working memory tasks and interestingly, with lack of insight, a very common phenomenon associated with schizophrenia (Bergé et al., 2011; Cropley et al., 2016; Ha et al., 2004; Kang et al., 2011; Shad and Keshavan, 2015). Generally, lack of insight is also thought to be correlated with positive symptom dimensions which might explain these overlapping findings (Pousa et al., 2017). Furthermore, cortical thickness of inferior temporal gyri and fusiform gyri exhibit the strongest reductions in patients with schizophrenia suggesting that these regions may indeed be strongly associated with the pathophysiology of schizophrenia (van Erp et al., 2018). Importantly, the regions identified here and by Padmanabhan et al. *do not* overlap with brain areas that typically have been identified to be more specifically associated with auditory hallucinations (superior and middle temporal gyri) highlighting the specificity of the association identified here between the symptom profile and structural GM alterations (Allen et al., 2012; Modinos et al., 2013).

Similar to the current findings, Padmanabhan and colleagues found fewer associations between cortical measures and the negative PANSS scale. They suggest that negative symptoms are to a lesser extent paralleled by cortical abnormalities. Here, only one item from the PANSS negative

scale (poor rapport) contributed to the PANSS component even though there was a moderate correlation between the negative scale and the PANSS component. Interestingly, this lack of widespread abnormalities associated with negative symptoms contrasts previous findings from univariate analysis (Koutsouleris et al., 2008) potentially highlighting higher specificity of multivariate approaches.

Higher GM concentration in sensorimotor cortices also contributed to the structural MRI component. However, previous studies have revealed decreases in GM concentration in individuals with schizophrenia relative to healthy controls in these brain regions (Ha et al., 2004; Ivleva et al., 2017; Narr et al., 2005). Interestingly though, neither study did investigate or observe an association with clinical symptoms whereas in the current study, relatively higher GM concentration in individuals with schizophrenia in sensorimotor cortices was associated with a specific pattern of PANSS items which might explain the different findings.

In our earlier work applying SBM analysis to GM concentration images (Gupta et al., 2015), we found similar anatomical regions as in the current study that were different between individuals with schizophrenia and age-matched controls. However, this study failed to identify an association between GM concentration and the PANSS positive score when applying post hoc correlation analyses. This observation highlights the advantage of the pICA approach: PANSS items and GM concentration images were analyzed simultaneously within the pICA framework and yielded a distinct set of PANSS items that were associated with structural brain features.

5. Conclusion

We extend previous findings of altered structural properties of GM in schizophrenia by highlighting an association between a distinct set of symptoms and patterns of GM concentration. Applying pICA we were able to reveal an association between delusional symptoms and suspiciousness and reductions of GM concentration in inferior temporal and fusiform gyri that has not been identified in previous analyses even when utilizing very similar data (Gupta et al., 2015). These findings may encourage future studies to apply similar higher-order statistical analyses to multi-modal data including various neuroimaging modalities and other clinical assessments or scales to identify patterns of abnormalities specific to a given dimension of psychopathology.

Author contribution statement

JAT and VDC devised the project. WJ and EM performed imaging and statistical analyses that JL and JAT advised on. EM and WJ wrote the manuscript in consultation with JAT. All coauthors provided critical feedback to improve the manuscript.

Conflict of interest

All authors declare that there are no conflicts of interest.

Funding sources

This research was funded by National Institutes of Health (NIH) R01MH094524 (JAT, VDC) and P20GM103472/P30GM122734 (VDC). WJ was supported in part by a Brains & Behavior fellowship through Georgia State University. The original data collection for FBIRN was supported by NIH 1 U24 RR021992 (Functional imaging Biomedical Information Research Network).

Acknowledgment

We thank all participants for their time to contribute to this study.

Appendix A. Supplementary data

Supplementary data to this article can be found online at https://doi.org/10.1016/j.schres.2019.02.010.

References

Aine, C.J., Bockholt, H.J., Bustillo, J.R., Cañive, J.M., Caprihan, A., Gasparovic, C., Hanlon, F.M., Houck, J.M., Jung, R.E., Lauriello, J., Liu, J., Mayer, A.R., Perrone-Bizzozero, N.I., Posse, S., Stephen, J.M., Turner, J.A., Clark, V.P., Calhoun, V.D., 2017. Multimodal neuroimaging in schizophrenia: description and dissemination. Neuroinformatics 15, 343–364. https://doi.org/10.1007/s12021-017-9338-9.

Allen, P., Modinos, G., Hubl, D., Shields, G., Cachia, A., Jardri, R., Thomas, P., Woodward, T., Shotbolt, P., Plaze, M., Hoffman, R., 2012. Neuroimaging auditory hallucinations in schizophrenia: from neuroanatomy to neurochemistry and beyond. Schizophr. Bull. 38, 695–703. https://doi.org/10.1093/schbul/sbs066.

American Psychiatric Association, et al., 2003. Diagnostic and Statistical Manual of Mental Disorders: DSM-5. ManMag.

Andreasen, N.C., Flaum, M., 1991. Schizophrenia: the characteristic symptoms. Schizophr. Bull. 17, 27–49. https://doi.org/10.1093/schbul/17.1.27.

Ashburner, J., Friston, K.J., 2000. Voxel-based morphometry—the methods. NeuroImage 11, 805–821. https://doi.org/10.1006/nimg.2000.0582.

Athanasiu, L., Mattingsdal, M., Kähler, A.K., Brown, A., Gustafsson, O., Agartz, I., Giegling, I., Muglia, P., Cichon, S., Rietschel, M., Pietiläinen, O.P.H., Peltonen, L., Bramon, E., Collier, D., St. Clair, D., Sigurdsson, E., Petursson, H., Rujescu, D., Melle, I., Steen, V.M., Djurovic, S., Andreassen, O.A., 2010. Gene variants associated with schizophrenia in a Norwegian genome-wide study are replicated in a large European cohort. J. Psychiatr. Res. 44, 748–753. https://doi.org/10.1016/j.jpsychires.2010.02.002.

Bell, A.J., Sejnowski, T.J., 1995. An information-maximization approach to blind separation and blind deconvolution. Neural Comput. 7, 1129–1159.

Bergé, D., Carmona, S., Rovira, M., Bulbena, A., Salgado, P., Vilarroya, O., 2011. Gray matter volume deficits and correlation with insight and negative symptoms in first-psychotic-episode subjects. Acta Psychiatr. Scand. 123, 431–439. https://doi.org/10.1111/j.1600-0447.2010.01635.x.

Birnbaum, R., Weinberger, D.R., 2017. Genetic insights into the neurodevelopmental origins of schizophrenia. Nat. Rev. Neurosci. 18, 727–740. https://doi.org/10.1038/nrn.2017.125.

Bora, E., 2015. Neurodevelopmental origin of cognitive impairment in schizophrenia. Psychol. Med. 45, 1–9. https://doi.org/10.1017/S0033291714001263.

Calhoun, V.D., Sui, J., 2016. Multimodal fusion of brain imaging data: a key to finding the missing link(s) in complex mental illness. Biol. Psychiatry Cogn. Neurosci. Neuroimaging, Brain Connectivity in Psychopathology 1, 230–244. https://doi.org/10.1016/j.bpsc.2015.12.005.

Cropley, V.L., Lin, A., Nelson, B., Reniers, R.L.E.P., Yung, A.R., Bartholomeusz, C.F., Klauser, P., Velakoulis, D., McGorry, P., Wood, S.J., Pantelis, C., 2016. Baseline grey matter volume of non-transitioned "ultra high risk" for psychosis individuals with and without attenuated psychotic symptoms at long-term follow-up. Schizophr. Res., Progressive Brain Tissue Loss in Schizophrenia 173, 152–158. https://doi.org/10.1016/j.schres.2015.05.014.

Cui, Y., Liu, B., Song, M., Lipnicki, D.M., Li, J., Xie, S., Chen, Y., Li, P., Lu, L., Lv, L., Wang, H., Yan, H., Yan, J., Zhang, H., Zhang, D., Jiang, T., 2018. Auditory verbal hallucinations are related to cortical thinning in the left middle temporal gyrus of patients with schizophrenia. Psychol. Med. 48, 115–122. https://doi.org/10.1017/S0033291717001520.

First, M.B., Gibbon, M., 2004. The Structured Clinical Interview for DSM-IV Axis I disorders (SCID-I) and the Structured Clinical Interview for DSM-IV Axis II disorders (SCID-II). In: Hilsenroth, M.J., Segal, D.L. (Eds.), Comprehensive Handbook of Psychological Assessment. Personality Assessment vol. 2. John Wiley & Sons Inc., Hoboken, NJ, US, pp. 134–143.

Fornito, A., Yücel, M., Patti, J., Wood, S.J., Pantelis, C., 2009. Mapping grey matter reductions in schizophrenia: an anatomical likelihood estimation analysis of voxel-based morphometry studies. Schizophr. Res. 108, 104–113. https://doi.org/10.1016/j.schres.2008.12.011.

Gerlach, C., Aaside, C.T., Humphreys, G.W., Gade, A., Paulson, O.B., Law, I., 2002. Brain activity related to integrative processes in visual object recognition: bottom-up integration and the modulatory influence of stored knowledge. Neuropsychologia 40, 1254–1267. https://doi.org/10.1016/S0028-3932(01)00222-6.

Glahn, D.C., Laird, A.R., Ellison-Wright, I., Thelen, S.M., Robinson, J.L., Lancaster, J.L., Bullmore, E., Fox, P.T., 2008. Meta-analysis of gray matter anomalies in schizophrenia: application of anatomic likelihood estimation and network analysis. Biol. Psychiatry 64, 774–781. https://doi.org/10.1016/j.biopsych.2008.03.031.

Gupta, C.N., Calhoun, V.D., Rachakonda, S., Chen, J., Patel, V., Liu, J., Segall, J., Franke, B., Zwiers, M.P., Arias-Vasquez, A., Buitelaar, J., Fisher, S.E., Fernandez, G., Erp, V., M, T.G., Potkin, S., Ford, J., Mathalon, D., McEwen, S., Lee, H.J., Mueller, B.A., Greve, D.N., Andreassen, O., Agartz, I., Gollub, R.L., Sponheim, S.R., Ehrlich, S., Wang, L., Pearlson, G., Glahn, D.C., Sprooten, E., Mayer, A.R., Stephen, J., Jung, R.E., Canive, J., Bustillo, J., Turner, J.A., 2015. Patterns of gray matter abnormalities in schizophrenia based on an international mega-analysis. Schizophr. Bull. 41, 1133–1142. https://doi.org/10.1093/schbul/sbu177.

Gur, R.C., Calkins, M.E., Satterthwaite, T.D., Ruparel, K., Bilker, W.B., Moore, T.M., Savitt, A.P., Hakonarson, H., Gur, R.E., 2014. Neurocognitive growth charting in psychosis spectrum youths. JAMA Psychiat. 71, 366. https://doi.org/10.1001/jamapsychiatry.2013.4190.

Ha, T.H., Youn, T., Ha, K.S., Rho, K.S., Lee, J.M., Kim, I.Y., Kim, S.I., Kwon, J.S., 2004. Gray matter abnormalities in paranoid schizophrenia and their clinical correlations. Psychiatry Res. Neuroimaging 132, 251–260. https://doi.org/10.1016/j.pscychresns.2004.05.001.

Hare, S.M., Ford, J.M., Ahmadi, A., Damaraju, E., Belger, A., Bustillo, J., Lee, H.J., Mathalon, D.H., Mueller, B.A., Preda, A., Erp, V., M, T.G., Potkin, S.G., Calhoun, V.D., Turner, J.A., 2017. Modality-dependent impact of hallucinations on low-frequency fluctuations in schizophrenia. Schizophr. Bull. 43, 389–396. https://doi.org/10.1093/schbul/sbw093.

Hare, S.M., Ford, J.M., Mathalon, D.H., Damaraju, E., Bustillo, J., Belger, A., Lee, H.J., Mueller, B.A., Lim, K.O., Brown, G.G., Preda, A., Potkin, S.G., Calhoun, V.D., Turner, J.A., 2018. Salience–default mode functional network connectivity linked to positive and negative symptoms of schizophrenia. Schizophr. Bull.

Harrison, P.J., 1999. The neuropathology of schizophrenia. A critical review of the data and their interpretation. Brain 122, 593–624. https://doi.org/10.1093/brain/122.4.593.

Himberg, J., Hyvärinen, A., 2003. Icasso: software for investigating the reliability of ICA estimates by clustering and visualization. Neural Networks for Signal Processing, 2003. NNSP'03. 2003 IEEE 13th Workshop On. IEEE, pp. 259–268.

Huhtaniska, S., Jääskeläinen, E., Hirvonen, N., Remes, J., Murray, G.K., Veijola, J., Isohanni, M., Miettunen, J., 2017. Long-term antipsychotic use and brain changes in schizophrenia – a systematic review and meta-analysis. Hum. Psychopharmacol. Clin. Exp. 32, e2574. https://doi.org/10.1002/hup.2574.

Ivleva, E.I., Clementz, B.A., Dutcher, A.M., Arnold, S.J.M., Jeon-Slaughter, H., Aslan, S., Witte, B., Poudyal, G., Lu, H., Meda, S.A., Pearlson, G.D., Sweeney, J.A., Keshavan, M.S., Tamminga, C.A., 2017. Brain structure biomarkers in the psychosis biotypes: findings from the bipolar-schizophrenia network for intermediate phenotypes. Biol. Psychiatry, Schizophrenia: Microstructure and Macrostructure 82, 26–39. https://doi.org/10.1016/j.biopsych.2016.08.030.

Kang, S.S., Sponheim, S.R., Chafee, M.V., MacDonald, A.W., 2011. Disrupted functional connectivity for controlled visual processing as a basis for impaired spatial working memory in schizophrenia. Neuropsychologia 49, 2836–2847. https://doi.org/10.1016/j.neuropsychologia.2011.06.009.

Kay, S.R., Flszbein, A., Opfer, L.A., 1987. The positive and negative syndrome scale (PANSS) for schizophrenia. Schizophr. Bull. 13, 261.

Kim, N.Y., Lee, S.M., Erlendsdottir, M.C., McCarthy, G., 2014. Discriminable spatial patterns of activation for faces and bodies in the fusiform gyrus. Front. Hum. Neurosci. 8. https://doi.org/10.3389/fnhum.2014.00632.

Koutsouleris, N., Gaser, C., Jäger, M., Bottlender, R., Frodl, T., Holzinger, S., Schmitt, G.J.E., Zetzsche, T., Burgermeister, B., Scheuerecker, J., Born, C., Reiser, M., Möller, H.-J., Meisenzahl, E.M., 2008. Structural correlates of psychopathological symptom dimensions in schizophrenia: a voxel-based morphometric study. NeuroImage 39, 1600–1612. https://doi.org/10.1016/j.neuroimage.2007.10.029.

Koutsouleris, N., Meisenzahl, E.M., Davatzikos, C., Bottlender, R., Frodl, T., Scheuerecker, J., Schmitt, G., Zetzsche, T., Decker, P., Reiser, M., et al., 2009. Use of neuroanatomical pattern classification to identify subjects in at-risk mental states of psychosis and predict disease transition. Arch. Gen. Psychiatry 66, 700–712.

Liu, J., Calhoun, V., 2007. Parallel independent component analysis for multimodal analysis: application to fMRI and EEG data. 2007 4th IEEE International Symposium on Biomedical Imaging: From Nano to Macro, pp. 1028–1031 https://doi.org/10.1109/ISBI.2007.357030 Presented at the 2007 4th IEEE International Symposium on Biomedical Imaging: From Nano to Macro.

Liu, J., Pearlson, G., Windemuth, A., Ruano, G., Perrone-Bizzozero, N.I., Calhoun, V., 2009. Combining fMRI and SNP data to investigate connections between brain function and genetics using parallel ICA. Hum. Brain Mapp. 30, 241–255. https://doi.org/10.1002/hbm.20508.

Meda, S.A., Ruaño, G., Windemuth, A., O'Neil, K., Berwise, C., Dunn, S.M., Boccaccio, L.E., Narayanan, B., Kocherla, M., Sprooten, E., Keshavan, M.S., Tamminga, C.A., Sweeney, J.A., Clementz, B.A., Calhoun, V.D., Pearlson, G.D., 2014. Multivariate analysis reveals genetic associations of the resting default mode network in psychotic bipolar disorder and schizophrenia. Proc. Natl. Acad. Sci. 201313093. https://doi.org/10.1073/pnas.1313093111.

Modinos, G., Costafreda, S.G., van Tol, M.-J., McGuire, P.K., Aleman, A., Allen, P., 2013. Neuroanatomy of auditory verbal hallucinations in schizophrenia: a quantitative meta-analysis of voxel-based morphometry studies. Cortex 49, 1046–1055. https://doi.org/10.1016/j.cortex.2012.01.009.

Mørch-Johnsen, L., Nesvåg, R., Jørgensen, K.N., Lange, E.H., Hartberg, C.B., Haukvik, U.K., Kompus, K., Westerhausen, R., Osnes, K., Andreassen, O.A., Melle, I., Hugdahl, K., Agartz, I., 2017. Auditory cortex characteristics in schizophrenia: associations with auditory hallucinations. Schizophr. Bull. 43, 75–83. https://doi.org/10.1093/schbul/sbw130.

Murray, R.M., Bhavsar, V., Tripoli, G., Howes, O., 2017. 30 years on: how the neurodevelopmental hypothesis of schizophrenia morphed into the developmental risk factor model of psychosis. Schizophr. Bull. 43, 1190–1196. https://doi.org/10.1093/schbul/sbx121.

Narr, K.L., Bilder, R.M., Toga, A.W., Woods, R.P., Rex, D.E., Szeszko, P.R., Robinson, D., Sevy, S., Gunduz-Bruce, H., Wang, Y.-P., DeLuca, H., Thompson, P.M., 2005. Mapping cortical thickness and gray matter concentration in first episode schizophrenia. Cereb. Cortex 15, 708–719. https://doi.org/10.1093/cercor/bhh172.

Padmanabhan, J.L., Tandon, N., Haller, C.S., Mathew, I.T., Eack, S.M., Clementz, B.A., Pearlson, G.D., Sweeney, J.A., Tamminga, C.A., Keshavan, M.S., 2015. Correlations between brain structure and symptom dimensions of psychosis in schizophrenia, schizoaffective, and psychotic bipolar I disorders. Schizophr. Bull. 41, 154–162. https://doi.org/10.1093/schbul/sbu075.

Pearlson, G.D., Calhoun, V.D., Liu, J., 2015. An introductory review of parallel independent component analysis (p-ICA) and a guide to applying p-ICA to genetic data and imaging phenotypes to identify disease-associated biological pathways and systems in common complex disorders. Front. Genet. 6. https://doi.org/10.3389/fgene.2015.00276.

Potkin, S.G., Turner, J.A., Brown, G.G., McCarthy, G., Greve, D.N., Glover, G.H., Manoach, D.S., Belger, A., Diaz, M., Wible, C.G., Ford, J.M., Mathalon, D.H., Gollub, R., Lauriello, J., O'Leary, D., Erp, V., M, T.G., Toga, A.W., Preda, A., Lim, K.O., 2009. Working memory and DLPFC inefficiency in schizophrenia: the FBIRN study. Schizophr. Bull. 35, 19–31. https://doi.org/10.1093/schbul/sbn162.

Pousa, E., Ochoa, S., Cobo, J., Nieto, L., Usall, J., Gonzalez, B., Garcia-Ribera, C., Pérez Solà, V., Ruiz, Ada-I, Baños, I., Cobo, J., García-Ribera, C., González, B., Massons, C., Nieto, L., Monserrat, C., Ochoa, S., Pousa, E., Ruiz, Ada-Inmaculada, Ruiz, I., Sanchez-Cabezudo, D., Usall, J., 2017. A deeper view of insight in schizophrenia: insight dimensions, unawareness and misattribution of particular symptoms and its relation with psychopathological factors. Schizophr. Res. 189, 61–68. https://doi.org/10.1016/j.schres.2017.02.016.

Samartzis, L., Dima, D., Fusar-Poli, P., Kyriakopoulos, M., 2014. White matter alterations in early stages of schizophrenia: a systematic review of diffusion tensor imaging studies: white matter alterations in early schizophrenia. J. Neuroimaging 24, 101–110. https://doi.org/10.1111/j.1552-6569.2012.00779.x.

Satterthwaite, T.D., Vandekar, S.N., Wolf, D.H., Bassett, D.S., Ruparel, K., Shehzad, Z., Craddock, R.C., Shinohara, R.T., Moore, T.M., Gennatas, E.D., Jackson, C., Roalf, D.R., Milham, M.P., Calkins, M.E., Hakonarson, H., Gur, R.C., Gur, R.E., 2015. Connectome-wide network analysis of youth with psychosis-spectrum symptoms. Mol. Psychiatry 20, 1508–1515. https://doi.org/10.1038/mp.2015.66.

Satterthwaite, T.D., Wolf, D.H., Calkins, M.E., Vandekar, S.N., Erus, G., Ruparel, K., Roalf, D.R., Linn, K.A., Elliott, M.A., Moore, T.M., Hakonarson, H., Shinohara, R.T., Davatzikos, C., Gur, R.C., Gur, R.E., 2016. Structural brain abnormalities in youth with psychosis spectrum symptoms. JAMA Psychiat. 73, 515–524. https://doi.org/10.1001/jamapsychiatry.2015.3463.

Shad, M.U., Keshavan, M.S., 2015. Neurobiology of insight deficits in schizophrenia: an fMRI study. Schizophr. Res. 165, 220–226. https://doi.org/10.1016/j.schres.2015.04.021.

Shinn, A.K., Pfaff, D., Young, S., Lewandowski, K.E., Cohen, B.M., Öngür, D., 2012. Auditory hallucinations in a cross-diagnostic sample of psychotic disorder patients: a descriptive, cross-sectional study. Compr. Psychiatry 53, 718–726. https://doi.org/10.1016/j.comppsych.2011.11.003.

Sun, H., Lui, S., Yao, L., Deng, W., Xiao, Y., Zhang, W., Huang, X., Hu, J., Bi, F., Li, T., Sweeney, J.A., Gong, Q., 2015. Two patterns of white matter abnormalities in medication-naive patients with first-episode schizophrenia revealed by diffusion tensor imaging and cluster analysis. JAMA Psychiat. 72, 678–686. https://doi.org/10.1001/jamapsychiatry.2015.0505.

Tandon, R., Gaebel, W., Barch, D.M., Bustillo, J., Gur, R.E., Heckers, S., Malaspina, D., Owen, M.J., Schultz, S., Tsuang, M., Van Os, J., Carpenter, W., 2013. Definition and description of schizophrenia in the DSM-5. Schizophr. Res. 150, 3–10. https://doi.org/10.1016/j.schres.2013.05.028.

Todtenkopf, M.S., Vincent, S.L., Benes, F.M., 2005. A cross-study meta-analysis and three-dimensional comparison of cell counting in the anterior cingulate cortex of schizophrenic and bipolar brain. Schizophr. Res. 73, 79–89. https://doi.org/10.1016/j.schres.2004.08.018.

Turner, J.A., Chen, H., Mathalon, D.H., Allen, E., Mayer, A., Abbott, C., Calhoun, V.D., Bustillo, J., 2012. Reliability of the amplitude of low-frequency fluctuations in resting state in chronic schizophrenia. Psychiatry Res. 201, 253–255. https://doi.org/10.1016/j.pscychresns.2011.09.012.

van Erp, T.G.M., Walton, E., Hibar, D.P., Schmaal, L., Jiang, W., Glahn, D.C., Pearlson, G.D., Yao, N., Fukunaga, M., Hashimoto, R., Okada, N., Yamamori, H., Bustillo, J.R., Clark, V.P., Agartz, I., Mueller, B.A., Cahn, W., de Zwarte, S.M.C., Hulshoff Pol, H.E., Kahn, R.S., Ophoff, R.A., van Haren, N.E.M., Andreassen, O.A., Dale, A.M., Doan, N.T., Gurholt, T.P., Hartberg, C.B., Haukvik, U.K., Jørgensen, K.N., Lagerberg, T.V., Melle, I., Westlye, L.T., Gruber, O., Kraemer, B., Richter, A., Zilles, D., Calhoun, V.D., Crespo-Facorro, B., Roiz-Santiañez, R., Tordesillas-Gutiérrez, D., Loughland, C., Carr, V.J., Catts, S., Cropley, V.L., Fullerton, J.M., Green, M.J., Henskens, F.A., Jablensky, A., Lenroot, R.K., Mowry, B.J., Michie, P.T., Pantelis, C., Quidé, Y., Schall, U., Scott, R.J., Cairns, M.J., Seal, M., Tooney, P.A., Rasser, P.E., Cooper, G., Shannon Weickert, C., Weickert, T.W., Morris, D.W., Hong, E., Kochunov, P., Beard, L.M., Gur, R.E., Gur, R.C., Satterthwaite, T.D., Wolf, D.H., Belger, A., Brown, G.G., Ford, J.M., Macciardi, F., Mathalon, D.H., O'Leary, D.S., Potkin, S.G., Preda, A., Voyvodic, J., Lim, K.O., McEwen, S., Yang, F., Tan, Y., Tan, S., Wang, Z., Fan, F., Chen, J., Xiang, H., Tang, S., Guo, H., Wan, P., Wei, D., Bockholt, H.J., Ehrlich, S., Wolthusen, R.P.F., King, M.D., Shoemaker, J.M., Sponheim, S.R., De Haan, L., Koenders, L., Machielsen, M.W., van Amelsvoort, T., Veltman, D.J., Assogna, F., Banaj, N., de Rossi, P., Iorio, M., Piras, F., Spalletta, G., McKenna, P.J., Pomarol-Clotet, E., Salvador, R., Corvin, A., Donohoe, G., Kelly, S., Whelan, C.D., Dickie, E.W., Rotenberg, D., Voineskos, A.N., Ciufolini, S., Radua, J., Dazzan, P., Murray, R., Reis Marques, T., Simmons, A., Borgwardt, S., Egloff, L., Harrisberger, F., Riecher-Rössler, A., Smieskova, R., Alpert, K.I., Wang, L., Jönsson, E.G., Koops, S., Sommer, I.E.C., Bertolino, A., Bonvino, A., Di Giorgio, A., Neilson, E., Mayer, A.R., Stephen, J.M., Kwon, J.S., Yun, J.-Y., Cannon, D.M., McDonald, C., Lebedeva, I., Tomyshev, A.S., Akhadov, T., Kaleda, V., Fatouros-Bergman, H., Flyckt, L., Farde, L., Flyckt, L., Engberg, G., Erhardt, S., Fatouros-Bergman, H., Cervenka, S., Schwieler, L., Piehl, F., Agartz, I., Collste, K., Victorsson, P., Malmqvist, A., Hedberg, M., Orhan, F., Busatto, G.F., Rosa, P.G.P., Serpa, M.H., Zanetti, M.V., Hoschl, C., Skoch, A., Spaniel, F., Tomecek, D., Hagenaars, S.P., McIntosh, A.M., Whalley, H.C., Lawrie, S.M., Knöchel, C., Oertel-Knöchel, V., Stäblein, M., Howells, F.M., Stein, D.J., Temmingh, H.S., Uhlmann, A., Lopez-Jaramillo, C., Dima, D., McMahon, A., Faskowitz, J.I., Gutman, B.A., Jahanshad, N., Thompson, P.M., Turner, J.A., 2018. Cortical brain abnormalities in 4474 individuals with schizophrenia and 5098 control subjects via the Enhancing Neuro Imaging Genetics Through Meta Analysis (ENIGMA) consortium. Biol. Psychiatry https://doi.org/10.1016/j.biopsych.2018.04.023.

Vergara, V.M., Ulloa, A., Calhoun, V.D., Boutte, D., Chen, J., Liu, J., 2014. A three-way parallel ICA approach to analyze links among genetics, brain structure and brain function. NeuroImage 98, 386–394. https://doi.org/10.1016/j.neuroimage.2014.04.060.

Vita, A., De Peri, L., Deste, G., Barlati, S., Sacchetti, E., 2015. The effect of antipsychotic treatment on cortical gray matter changes in schizophrenia: does the class matter? A meta-analysis and meta-regression of longitudinal magnetic resonance imaging studies. Biol. Psychiatry, Molecular Mechanisms for Synaptic Deficits in Schizophrenia 78, 403–412. https://doi.org/10.1016/j.biopsych.2015.02.008.

Walton, E., Hibar, D.P., van Erp, T.G.M., Potkin, S.G., Roiz-Santiañez, R., Crespo-Facorro, B., Suarez-Pinilla, P., Haren, N.E.M.V., de Zwarte, S.M.C., Kahn, R.S., Cahn, W., Doan, N.T., Jørgensen, K.N., Gurholt, T.P., Agartz, I., Andreassen, O.A., Westlye, L.T., Melle, I., Berg, A.O., Mørch-Johnsen, L., Færden, A., Flyckt, L., Fatouros-Bergman, H., Jönsson, E.G., Hashimoto, R., Yamamori, H., Fukunaga, M., Preda, A., Rossi, P.D., Piras, F., Banaj, N., Ciullo, V., Spalletta, G., Gur, R.E., Gur, R.C., Wolf, D.H., Satterthwaite, T.D., Beard, L.M., Sommer, I.E., Koops, S., Gruber, O., Richter, A., Krämer, B., Kelly, S., Donohoe, G., McDonald, C., Cannon, D.M., Corvin, A., Gill, M., Giorgio, A.D., Bertolino, A., Lawrie, S., Nickson, T., Whalley, H.C., Neilson, E., Calhoun, V.D., Thompson, P.M., Turner, J.A., Ehrlich, S., 2017. Positive symptoms associate with cortical thinning in the superior temporal gyrus via the ENIGMA Schizophrenia consortium. Acta Psychiatr. Scand. 135 (5), 439–447. https://doi.org/10.1111/acps.12718.

Walton, E., Hibar, D.P., van Erp, T.G.M., Potkin, S.G., Roiz-Santiañez, R., Crespo-Facorro, B., Suarez-Pinilla, P., van Haren, N.E.M., de Zwarte, S.M.C., Kahn, R.S., Cahn, W., Doan, N.T., Jørgensen, K.N., Gurholt, T.P., Agartz, I., Andreassen, O.A., Westlye, L.T., Melle, I., Berg, A.O., Morch-Johnsen, L., Færden, A., Flyckt, L., Fatouros-Bergman, H., Consortium (KaSP), K.S.P, Jönsson, E.G., Hashimoto, R., Yamamori, H., Fukunaga, M., Jahanshad, N., Rossi, P.D., Piras, F., Banaj, N., Spalletta, G., Gur, R.E., Gur, R.C., Wolf, D.H., Satterthwaite, T.D., Beard, L.M., Sommer, I.E., Koops, S., Gruber, O., Richter, A., Krämer, B., Kelly, S., Donohoe, G., McDonald, C., Cannon, D.M., Corvin, A., Gill, M., Giorgio, A.D., Bertolino, A., Lawrie, S., Nickson, T., Whalley, H.C., Neilson, E., Calhoun, V.D., Thompson, P.M., Turner, J.A., Ehrlich, S., 2018. Prefrontal cortical thinning links to negative symptoms in schizophrenia via the ENIGMA consortium. Psychol. Med. 48, 82–94. https://doi.org/10.1017/S0033291717001283.

Wible, C.G., Lee, K., Molina, I., Hashimoto, R., Preus, A.P., Roach, B.J., Ford, J.M., Mathalon, D.H., McCarthey, G., Turner, J.A., Potkin, S.G., O'Leary, D., Belger, A., Diaz, M., Voyvodic, J., Brown, G.G., Notestine, R., Greve, D., Lauriello, J., 2009. fMRI activity correlated with auditory hallucinations during performance of a working memory task: data from the FBIRN Consortium study. Schizophr. Bull. 35, 47–57. https://doi.org/10.1093/schbul/sbn142.

Xu, L., Groth, K.M., Pearlson, G., Schretlen, D.J., Calhoun, V.D., 2009. Source-based morphometry: the use of independent component analysis to identify gray matter differences with application to schizophrenia. Hum. Brain Mapp. 30, 711–724. https://doi.org/10.1002/hbm.20540.

Zhang, X.Y., Fan, F.M., Chen, D.C., Tan, Y.L., Tan, S.P., Hu, K., Salas, R., Kosten, T.R., Zunta-Soares, G., Soares, J.C., 2016. Extensive white matter abnormalities and clinical symptoms in drug-naive patients with first-episode schizophrenia: a voxel-based diffusion tensor imaging study. J. Clin. Psychiatry 77, 205–211. https://doi.org/10.4088/JCP.14m09374.